The Primary Role of Solar-Ultraviolet-Energy-Absorbing Gases in Global Warming

Peter L. Ward[1]

Abstract

The most energetic solar radiation reaching the earth's surface in substantial quantities is in the 0.3-0.4μm ultraviolet band containing 14% of solar energy. One molecule of sulfur dioxide (SO_2) in the lower troposphere absorbs as much of this energy as >42,000 molecules of carbon dioxide (CO_2) absorb in the much wider infrared band most strongly absorbed by CO_2 (12.7-17.5μm). Similarly, nitrogen dioxide, tropospheric ozone, and black carbon accompanying SO_2 in polluted air are strong absorbers of ultraviolet and visible energy. Rapid increases in anthropogenic pollution from 1950 to 1979, decreases to 2002 and increases again are reflected, with appropriate time delays, by changes in global temperatures, methane concentrations, global dimming, Arctic haze, acid rain, and tree-ring growth while annual CO_2 concentrations increased monotonically. The major warming effects of solar-ultraviolet-energy-absorbing gases described in this paper imply that we can reduce global warming economically using existing technology but should be verified experimentally.

[1] U.S. Geological Survey, retired, Teton Tectonics, P.O. Box 4875, Jackson, WY 83001, USA. E-mail: peward@wyoming.com, www.tetontectonics.org

Introduction

Many climatologists are convinced that sulfur dioxide (SO_2) does not increase global warming because:

1. SO_2 ejected into the stratosphere by large volcanic eruptions forms an aerosol that reflects sunlight and cools the earth for several years,
2. the concentration of CO_2 is ~9,000 times greater than the largest regional concentration of SO_2,
3. SO_2 from anthropogenic pollution is concentrated in specific layers and regions minimizing global impact,
4. SO_2 remains in the atmosphere for weeks while greenhouse gases remain for decades to centuries.

What is not well explained includes observations that:

1. regional concentrations of SO_2 accumulated to as much as 43 ppbv in specific regions peaking in the early 1980s (*1*),
2. background concentrations of sulfate in the snows of central Greenland similarly peaked in the 1970s (*2*),
3. yearly anthropogenic SO_2 emissions increased from 4.6 Mt in 1850 to a peak of 137 Mt in 1979 (*3*),
4. SO_2 from East Asia in 2006 accounted for 56% of sulfur measured over British Columbia (*4*) and was detectable in Europe within 8-12 days of emission (*5*),

5. the 14 periods of most rapid warming between 48,000 and 11,000 BP are contemporaneous with the 14 most prolonged concentrations of sulfate measured in ice cores from Summit Greenland (*2*, *6*),
6. volcanic SO_2 warms the stratosphere ~3^{o}C (*7*),
7. stratospheric temperatures are maintained as much as 50^{o}C above temperatures at the tropopause by <8 ppmv ozone (O_3) and related exothermic photochemical reactions.

These observations suggest that our understanding of global warming is incomplete.

The Physics of Global Warming

The globe is warmed when increased concentrations of radiatively active gases absorb energy of oscillation from the massless oscillations that constitute electromagnetic radiation (EMR). Atoms and molecules have precise normal modes of oscillation for each spatial degree of freedom defined by their atomic and molecular structures. Each normal mode absorbs only the frequency components of energy that are very close to its precise natural frequency through high Q-factor resonance when the intensity of any of their internal oscillations is less than the spectral intensity at identical frequencies in the EMR. EMR, on the other hand, absorbs energy from atoms and molecules when the spectral intensity of any of its internal oscillations is less than the intensity at identical frequencies in matter. EMR is the flow through space of the thermal energy of oscillation between bodies of matter. Energy is transferred only from warmer to cooler bodies and the amount of energy transferred increases with temperature gradient. (See the supporting online text for more detail.)

Planck's law (*8*) predicts the spectral intensity of radiation from the sun heated by nuclear fusion to 5525 K (Figure 1, red line) and the spectral intensity of radiation from the earth heated to 260 K primarily by solar radiation (blue line). The red and blue shaded areas show the effects of atmospheric absorption: the spectral intensities of solar radiation measured at the earth's surface and radiation from the earth measured at the top of the atmosphere. The spectral intensities have been normalized for comparison; the flux density averages ~1366 W/m^2 from the sun at the top of the daytime atmosphere and ~396 W/m^2 from earth (*9*). The percent of total absorption and scattering is shown in gray along with contributions from major components (*10*).

Since 1872 (*11*), attention has been focused on greenhouse gases absorbing infrared energy from the earth because water, CO_2, methane and other greenhouse gases are the most voluminous radiatively active gases in the atmosphere. But increase in temperature is a direct function of the oscillatory energy absorbed and Planck (*8*) showed that the minimum energy absorbed, the "size" of a photon at a specific frequency, is equal to the frequency times Planck's constant (dashed green line, Figure 1). Thus one molecule of SO_2 absorbing one photon of ultraviolet energy in the orange-shaded band absorbs ~50 times the energy (2.07 eV) of one molecule of CO_2 in the 14.9 μm band (0.0416 eV).

In addition, CO_2 absorbs along spectral lines (Figure 2) while solar-ultraviolet-energy-absorbing gases absorb along a continuum (SO_2 and O_3 in Figure 3, NO_2 in Figure S3). Total absorption in a specific waveband is the area under these lines/curves over the waveband of interest. For SO_2, data were collected at wavenumber intervals of

0.5 cm^{-1} (*12, 13*). Multiplying the intensity at each measured wavenumber by 0.5 and summing between 0.295 and 0.417 μm gives 8.92 x 10^{-16} cm^2/molecule. Assuming the spectral lines for CO_2 have a Lorenz line shape, the area under each line is twice the air-broadened half-width at half-maximum (*14*) times the line height times π/4 (*15*) and the sum across all spectral lines over the broader wavelength band from 12.7 to 17.5 μm is only 1.06 x 10^{-18} cm^2/molecule. Thus one molecule of SO_2 absorbs as many photons as ~841.5 molecules of CO_2 and since the energy of each photon is 50 times greater, one molecule of SO_2 absorbs as much oscillatory energy as >42,000 molecules of CO_2. In other words, ~9 ppbv SO_2 absorbs the same total oscillatory energy as 388 ppmv CO_2.

SO_2 is an easily observed species causing acid rain and leaving a sulfate history in glacial ice that indicates far more complex atmospheric chemistry, the sum of which appears to cause global warming. NO_2 and related tropospheric O_3 are the most important other gases associated with SO_2 in polluted environments that absorb substantial amounts of energy at both ultraviolet and visible wavelengths (λ) (Figures 3 and S3). Similarly black carbon, especially when entrained in aerosols, causes substantial heating (*16*).

Absorption by CO_2 is calculated by integrating throughout the whole atmospheric column while pollution is observed concentrated only in thin layers, but there are many reasons why absorption of energy in the ultraviolet and visible probably still leads to more intense warming than absorption in the infrared:

1. Rayleigh scattering becomes much more important at higher frequencies (Figure 1) causing more energy to be absorbed as the rays travel up and down within layers of gas,

2. the ultraviolet band between 0.3 and 0.4 μm contains 14% of solar energy (*17*) and most of it normally reaches the earth's surface (actinic flux, Figure 3),
3. most solar-ultraviolet-energy-absorbing gases have permanent electric dipoles making them more radiatively interactive with EMR, while CO_2 and methane do not,
4. gas molecules in the atmosphere "see" solar irradiance during the day that is 3.4 times more intense than the infrared irradiance seen from the earth and "see" the sun for more than 12 hours, especially during polar summers,
5. the "wavefront" of solar radiation travels obliquely through the atmosphere during the morning and afternoon, increasing the probability of absorption,
6. energy is absorbed and redistributed by collisions most efficiently at the increased densities, pressures, and rates of collision in the lowermost polluted troposphere,
7. fluorescence is observed sometimes when electronic transitions are involved ($\lambda <\sim 1$ μm) re-radiating lower frequency energy closer to the visible spectrum absorbed strongly by NO_2 and O_3,
8. molecules warmed by absorbing ultraviolet and visible energy radiate infrared energy absorbed by greenhouse gases,
9. the warming caused by layers of solar-energy-absorbing aerosols or gases increases with proximity to the earth's surface (*18*).

All of these issues and calculations suggest that ultraviolet-energy-absorbing gases are capable of causing global warming and may be more important than greenhouse gases as also suggested by the observations discussed below. Since more precise theoretical

calculations involve many assumptions, it would be much more direct to observe experimentally the precise increases in temperature caused by different trace gases under tropospheric conditions.

Atmospheric Lifetime of SO_2

It is widely assumed that SO_2 is readily oxidized to form sulfuric acid aerosols that cool the earth (*19*), but oxidation takes weeks. In 2006, West of Ireland, ~1 ppbv SO_2 from East Asia was measured at 5-7 km altitude having travelled 20,000 km in 8-12 days (*20*) and ~3 ppbv SO_2 from North America was concentrated at 1-2 km (*5, 21*). The e-folding time to oxidize 37% of Asian SO_2 appears to have been 7-14 days (*5*). When 17 Mt SO_2 was added suddenly to the stratosphere by the eruption of Pinatubo in 1991, it took 21 days to circle the globe but 35 days to oxidize 37% (*22*). SO_2 in this layer was still detectable by satellite after 170 days (*23*). Oxidation rate is set primarily by the demand for and amount of the hydroxyl radical (OH) available. OH is formed from ozone in a sequence initiated by ultraviolet energy ($\lambda<0.32$ μm), both of which are less available in the troposphere than in the stratosphere. But ozone mixing ratios can be enhanced by NO_x pollution. Model simulation suggests that nitrogen associated with the East Asian pollution layer observed at altitudes of 2-4 km just west of North America enhanced surface ozone concentrations 5-7 ppb (*24*).

Anthropogenic pollution is often lifted into the upper troposphere by warm conveyor belts associated with cyclonic systems and by deep convection in clouds. Models confirm the unexpected observations that <1.5% SO_2 is permanently depleted during such updrafts even in wet clouds (*21, 25, 26*). Fiedler et al. (*20*) described in

considerable detail the path of pollution from East Asia to Ireland emphasizing the complex and inefficient ways SO_2 is slowly oxidized. Furthermore in the lowest troposphere dry deposition of SO_2 appears to be far more effective than wet deposition under most circumstances (see supporting online text).

When SO_2 is oxidized, all aerosols are not created equal. Volcanic SO_2 in the stratosphere forms nearly pure aerosols (59-77% H_2SO_4 in water)(*27*) at temperatures <-50^oC that scatter sunlight before it can enter the troposphere containing >80% of the mass of the atmosphere. Aerosols formed in the troposphere, however, typically contain impurities such as black carbon or volcanic ash that absorb substantial amounts of solar energy (*16*) and scatter solar energy throughout polluted layers containing SO_2, NO_2, O_3, black carbon, etc.

When pollution is emitted continuously, the "lifetime" of SO_2 at any distance from the source lasts as long as the pollution is emitted. While weather systems may distribute the SO_2 in ways that change oxidation rates, there are long-term average concentrations observed to increase as pollution increases.

The Importance of the Ocean to Global Warming

The mean temperature of the earth's surface, which increased ~0.8^oC over the past century (*28*), is closely related to the mean temperature of the ocean surface covering 71% of the earth. The ocean provides the primary heat capacity in the climate system (*29*). The heat capacity of the whole atmosphere is equal to the heat capacity of ~3.2 meters of the ocean, yet the average depth of the ocean is 3800 meters (*30*). Thus global

warming requires warming the ocean. Equatorial Pacific sea surface temperatures during the last glacial maximum were ~3^{o}C lower than today (*31*).

The globe warms when infrared radiation from the earth's surface into space cannot keep pace with surface warming by the sun. The intensity or rate of infrared radiation increases with increasing temperature gradient (lapse rate). Radiation at night is considerable from hot rocks baked in the sun where daytime heat is not conducted efficiently down into the earth. But in the ocean, daytime heat is readily conducted or mixed down from the surface. Most solar radiation absorbed on land is re-radiated overnight; most solar radiation at sea is absorbed until the whole mixed-layer of the ocean (25-200m) is warmed. Several model simulations do suggest that recent warming over land occurred largely in response to warming oceans rather than as a direct response to increasing greenhouse gases over land (*32-34*).

If gases in the lowermost troposphere above the ocean absorbed enough energy to warm even a thin atmospheric layer to the temperature at the ocean's surface, there would, in the steady state, be no radiation of energy from the ocean, only upward radiation from the top of the gas layer. Thus gases warming the lowermost troposphere have a greater effect decreasing surface emission and increasing global warming than gases warming the whole troposphere to a slightly lower temperature as commonly assumed when modeling the total column of well-mixed gases such as CO_2 and methane. A cloudy sky similarly reduces the temperature gradient, reducing surface radiation as well as insolation. Of course diurnal temperature variations, convection, and latent heat complicate the details.

But what is an appropriate time constant for warming the ocean? Thin layers of SO_2 pollution in the lower stratosphere are well observed and modeled to decrease ocean temperatures by scattering sunlight. Climate models (*35*-*37*) show that cooling the ocean surface for three years after a volcanic eruption will have thermal effects on ocean temperature over periods of 10-100 years depending on the size of the eruption and the depth of water affected (*30*) and that a sequence of large explosive volcanic eruptions spaced out over decades can incrementally cool the ocean (*6*). Data plotted in Figure 6 and described below imply that the rapid and continuous increase in SO_2 emissions and related pollution in the lower troposphere especially in northern mid-latitudes from 1950 to 1980 is reflected in the increase of ocean-surface temperature ~30 years later, an appropriate time delay within the range of delays in cooling mentioned above. Direct modeling is needed.

Evidence for Atmospheric Heating by Solar-Ultraviolet-Energy-Absorbing Gases

Less than 8 ppmv ozone at altitudes of 15-50 km (*38*) absorbs most of the higher energy solar ultraviolet radiation with wavelengths <0.3 μm, protecting life on earth from this damaging radiation. This absorption plus related exothermic chemical processes for creating and destroying ozone raise atmospheric temperatures as much as 50^{o}C above the temperature at the tropopause, forming and maintaining a temperature inversion we call the stratosphere, a warming effect orders of magnitude greater than attributed to all tropospheric gases and aerosols combined. Lower densities in the stratosphere make warming easier, but also mean there are far fewer molecules of ozone absorbing much larger photons of energy (>4.13 eV).

The most direct and unequivocal observation of SO_2-caused warming followed the June 8, 1783, eruption of Laki in southern Iceland, one of the most effusive basaltic volcanic eruptions in written history (*39*, *40*). Basaltic volcanoes typically emit 10 to 100 times more SO_2 per volume magma erupted (*41*) than volcanoes with more evolved magmas and are not particularly explosive, emitting SO_2 primarily into the troposphere. Laki erupted 24 Mt SO_2 into the stratosphere where it was carried eastward and northward but 98 Mt into the troposphere where it was carried southeastward to Europe (*39*, *40*). A haze or "dry fog" settled over Europe by June 26, raising daytime temperatures as much as 3.3^{o}C compared to long-term means, causing severe acid damage to vegetation from Iceland to Finland to Italy, and killing more than 50,000 people. The "dry fog" was primarily SO_2 and fine ash based on the respiratory effects on humans, the acid effects on vegetation, a faint smell at times detectable by most humans at concentrations of 300 to 1000 ppbv (*42*), and made visible by ultrafine volcanic ash, Rayleigh scattering and fluorescence causing an observed bluish tinge. There were ten eruptive phases that kept the density of "dry fog" from moderate to high for four months. In central England, 1783 was the warmest July on record from the earliest data in 1659 until 1983 (*43*, *44*).

Atmospheric concentrations of SO_2 are recorded by sulfate deposits in snow falling in Greenland (*2*) (Figure 4). "Volcanic" sulfate is total measured sulfate per layer (~1.8 years) minus that attributed to continental dust and sea salt (*45*) and includes anthropogenic sulfate during the 20th century. The circled numbers show the number of contiguous layers of snow containing sulfate, a measure of how continuous volcanism

was. Continuity is important, for the buildup and duration of SO_2 pollution and thus the amount and duration of warming. The highest and most continuous concentrations of this sulfate prior to the 20th century were contemporaneous with and occurred only during periods of most rapid warming at the end of the last ice age and during all 14 Dansgaard-Oeschger abrupt climate warmings between 48,000 and 10,000 years (*6*, *46*). The sulfate deposits, at least during the Bolling and Preboreal warmings, indicate volcanism at rates ~100 times greater than observed in written history. While individual large explosive volcanic eruptions inject SO_2 into the stratosphere where it is converted to aerosols that reflect sunlight and cool the earth for a few years, very frequent and likely more basaltic eruptions appear to maintain a level of SO_2 in the troposphere that causes warming. In the case of the Dansgaard-Oeschger abrupt warmings, volcanic SO_2 emissions ended typically within decades or centuries, before the temperature of the ocean warmed, so the oceans cooled the world back into an ice age (*6*). But major volcanism during the Preboreal warming continued for more than 2000 years, sufficient to warm the ocean out of the last ice age. The relationship between volcanic activity and Milankovitch cycles is discussed elsewhere (*6*).

During the 20th century, sulfate deposits in Greenland were at least as large as during the Preboreal warming (Figure 4), but the source of SO_2 was anthropogenic. Anthropogenic sulfur emissions (black line, Figure 5) (*3*) increased rapidly until 1979 as did the background level of sulfate (red bars). Trace element analyses of the background sulfate show that most originated in northern Europe and Asia with sporadic contributions from mid-western North America (*47-49*). For the 2000 years before 1850,

76% of the layers contained no residual sulfate, yet all 34 layers since 1928 contain sulfate, the most number of contiguous layers since the Preboreal warming.

Regulations in several nations aimed at reducing acid rain led to a 20% decrease in global anthropogenic sulfur emissions between 1979 and 2002 primarily through installation of SO_2 scrubbers in smokestacks, more efficient techniques for burning coal, and substitution of North Sea oil for coal. But by 2003, rapid increase in the number of coal-burning power plants in Asia caused global emissions to increase again. These two major inflection points in the anthropogenic sulfur curve during 1979 and 2003 (black arrows in Figure 6) are observable in several aspects of climate change:

1. Temperatures in the northern hemisphere (red line) and southern hemisphere (dashed red line) increased rapidly (with a delay of ~30 years to warm the ocean) as SO_2 emissions increased but the rate of increase approached zero by 1998 as SO_2 emissions decreased. The increase was greatest by nearly a factor of two in the northern hemisphere where 94% of coal (*3*), the primary source of anthropogenic SO_2, was consumed.
2. SO_2 and methane are primarily oxidized by OH, formed from O_3 by ultraviolet radiation. But O_3 and OH are in limited supply in the troposphere and SO_2 reacts with OH more quickly than methane. The rate of increase in methane concentrations (green line) decreased to zero by 2002 as SO_2 emissions decreased but began increasing again in 2007 (*50*) as SO_2 emissions began to increase. Thus the increase in methane since 1950 is likely due to a reduction in the ability of the

atmosphere to oxidize and remove methane rather than an increase in methane emissions.

3. Global dimming (*51*), the decrease in solar radiation at the earth's surface (purple line), increased rapidly in Europe once SO_2 emissions remained high and reduced as soon as SO_2 emissions decreased substantially. Much more intense regional dimming was well observed in Europe when concentrations of SO_2 and fine ash were high following the Laki eruption (*40*). Dimming in East Asia increased after 2000 in phase with local dramatic increases in SO_2 emissions (*52*).
4. Tree ring density and thickness normally increase with temperature, but since the 1940s these measures have diverged in northern forests (*53*). SO_2 is well-known to stress and even kill trees (*54, 55*). When anthropogenic SO_2 levels began to decline in the early 1980s, wide-spread greening in northern regions was observed from satellites (*56*).

The atmospheric concentration of CO_2 (blue line), meanwhile, increased throughout the 20th century with no major long-term inflection points (*57*). Current scientific consensus is that a doubling of CO_2 concentrations would most likely cause warming of ~3^{o}C (*19*). But this linear relationship clearly does not apply to temperatures since 1998 that have remained relatively constant with approximately equal peaks in 1998, 2005, and 2010 during El Niño years (*58*).This may be one reason why global climate models based on CO_2 absorption overestimate global warming since 1998 (*59, 60*) and are probably overestimating warming in future decades. A temporal relationship

between temperature and concentrations of CO_2 is well observed in ice cores over the past 800,000 years (*61*), but a cold ocean absorbs more CO_2 (*62*) and detailed studies (*63-68*) conclude that the release of most CO_2 follows the warming by hundreds to a few thousand years. Other issues related to CO_2 are discussed in the supporting online text.

All aspects of climate change in the past 80 years enumerated above show logical temporal relationships to changes in anthropogenic pollution associated with SO_2, but not to monotonically increasing concentrations of CO_2. All known periods of major warming in the past 40,000 years are similarly contemporaneous with increases in SO_2 and related pollution but precede increases in CO_2 (*6*). Such temporal relationships should be explored using general climate models.

Conclusion and Ways to Verify the Thermal Effects of SO_2

Theory and observations strongly imply that solar-ultraviolet-energy-absorbing gases and associated black carbon play the primary role in global warming, that anthropogenic pollution played the primary role in 20th century global warming, and that volcanic pollution of similar amounts played the primary role during earlier periods of abrupt global warming. These deductions can be verified in at least three ways.

The greatest need is for experimental studies that measure and contrast the actual heat generated when SO_2, NO_2, O_3, water, CO_2, and methane absorb ultraviolet and infrared radiant energy under lower tropospheric conditions.

The best natural laboratory for studying the thermal effects of pollution is within or downwind from Asia. Between 2000 and 2005, anthropogenic emissions of SO_2 rose

53% in China, 17% in India, and 24% for shipping worldwide, with a global increase of 8% (*3*). One-third of China's land area is affected by acid rain causing damage totaling ~1% Gross Domestic Product (*1*). Hundreds of thousands of people in China die prematurely each year because of widespread air pollution (*69*). China has an aggressive cap-and-trade program to reduce SO_2 emissions that brought about a decrease in emissions after 2006 (*52*). Simultaneous measurements of solar energy attenuation at different levels in the troposphere downwind from the most polluted areas of China and India should demonstrate the thermal effects of SO_2 and related pollution, although the red bars in Figure 5 suggest that concentrations, at least at a distance, are likely to fall very rapidly when continuous emissions are no longer increasing.

Global climate models need to be updated to include absorption of pollution in the visible and ultraviolet bands and to evaluate the effects of thin layers of pollution on ocean warming. Warming due to Asian pollution observed spanning the oceans coupled with a severe El Niño need to be modeled to see if they can help explain the unusually high precipitation and energetic storminess observed in North America during 2010-2011.

If pollution evidenced by SO_2 was the primary cause of 20^{th} century global warming, as proposed here, then we know how to control global warming economically; we have apparently done so unintentionally by trying to reduce acid rain. The problem is, we have no proven way to cool the ocean rapidly back to pre-industrial temperatures and are therefore burdened with a warmer ocean and lowermost troposphere.

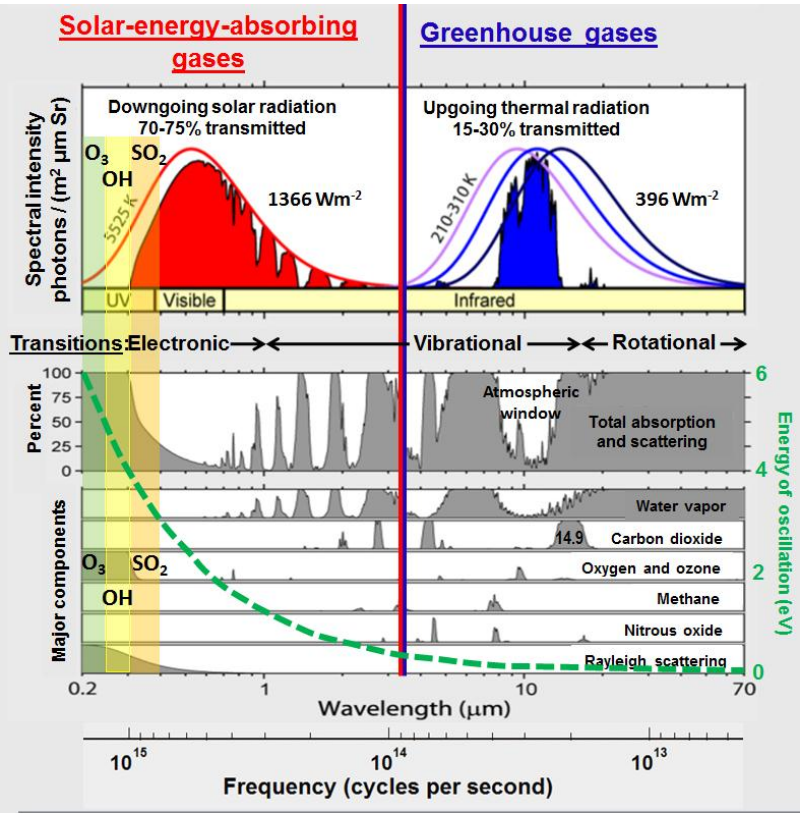

Fig. 1. SO_2 in the troposphere absorbs the highest energy solar ultraviolet radiation (orange shading) available after higher energy UV forms O_3 from O_2 (green) and OH from O_3 (yellow) (70). The absorption cross sections for O_3 and SO_2 are shown in more detail in Figure 3.

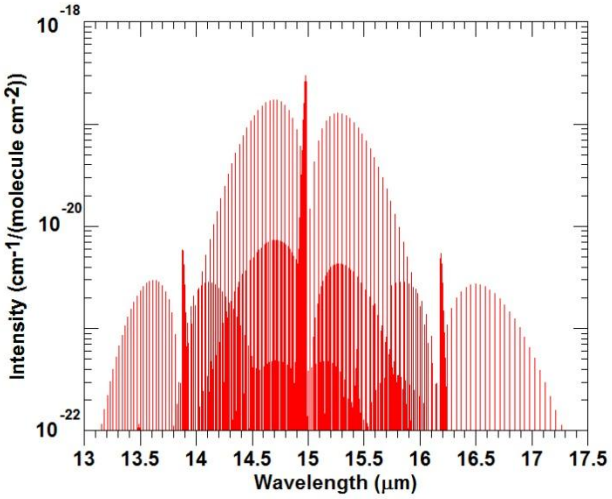

Fig. 2. Absorption of infrared EMR by CO_2 is very selective along spectral lines (14).

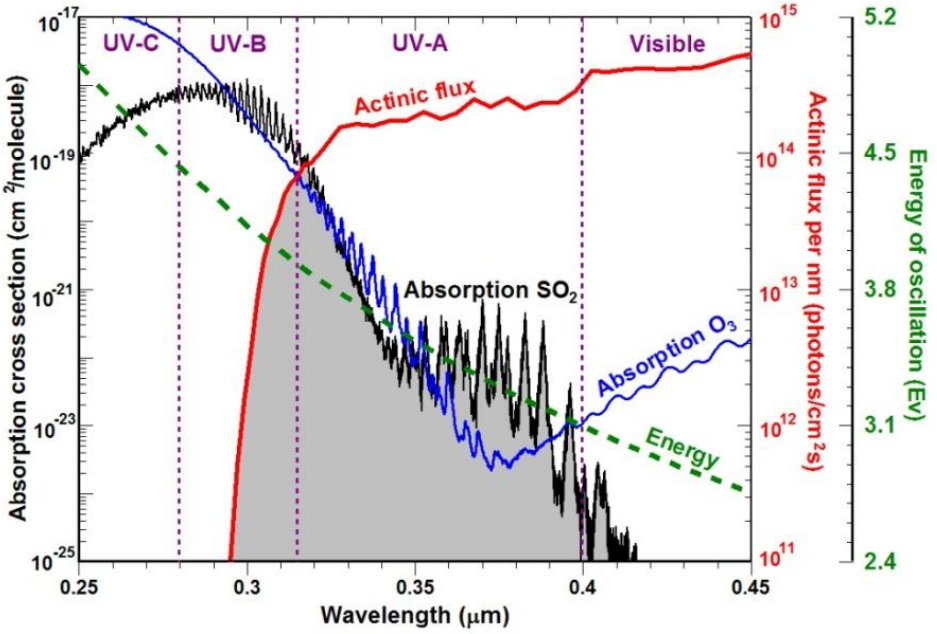

Fig. 3. SO_2 (black line)(13) absorbs the highest energy ultraviolet solar radiation that reaches the earth's surface defined by the actinic flux (red line) (70, 71). Energy (green line) is the minimum amount of energy absorbed per unit wavelength. Ozone (blue line, (14)) concentration in the troposphere is minimal except in polluted environments.

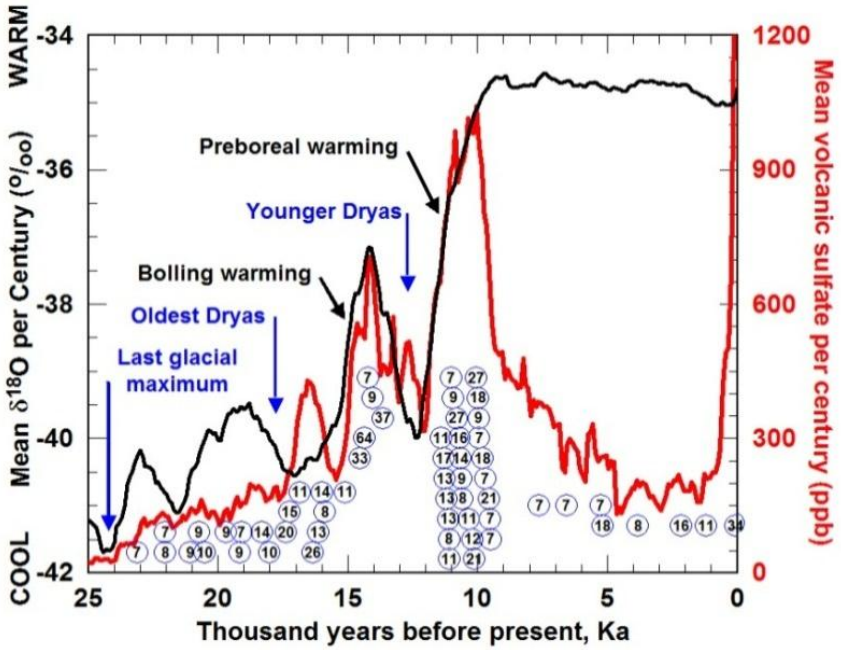

Fig. 4. Times of most rapid warming (black line) (*72*) at the end of the last ice age are contemporaneous with times of greatest volcanic sulfate in the GISP2 ice core (red line)(*2*). Numbers in circles show the continuity of volcanism, the number of contiguous layers in the ice core that contain volcanic sulfate, highest between 12 and 10 Ka when the ocean was warmed out of the ice age. The amount of SO_2 precipitated during the 20th century by humans burning fossil fuels was similar to the greatest amounts at the end of the last ice age. Both temperature proxy and sulfate per century have been smoothed with a symmetric eleven century running mean tapered to zero. Unsmoothed data are plotted elsewhere (*6*).

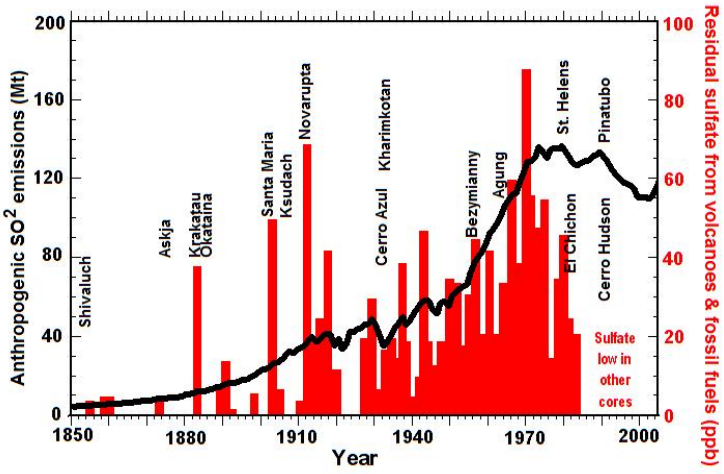

Fig. 5. Increases in anthropogenic sulfur emissions (black line) (3) and background level of residual sulfate (red bars) (2) near Summit Greenland are contemporaneous. Individual long bars are associated with known volcanic eruptions whose names are shown.

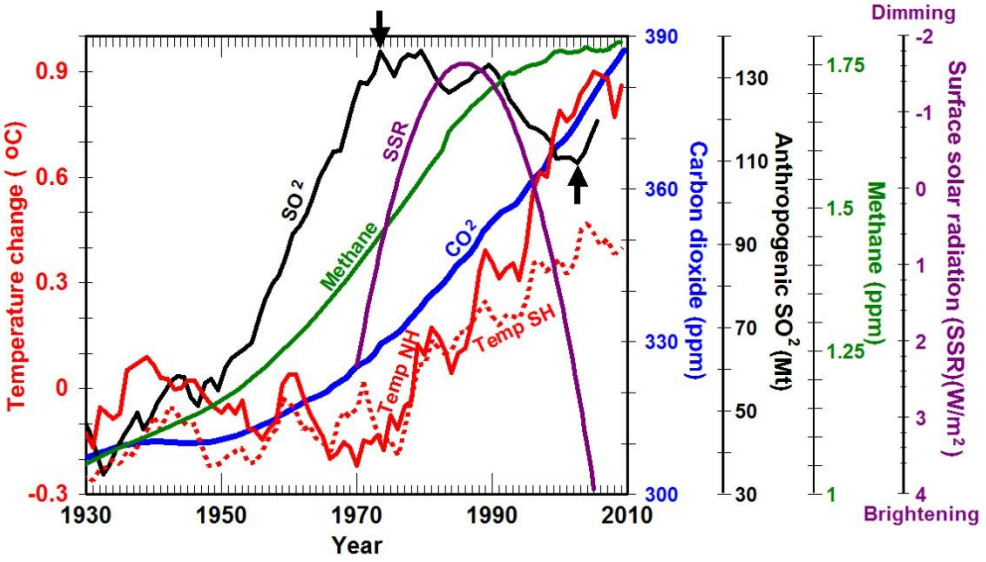

Fig. 6. The rapid increase in anthropogenic SO_2 emissions until 1979 (black line)(*3*), the 20% decrease by 2002, and the subsequent increase appear related to the rapid increases and decreases in the growth rate of methane concentrations (green line) (*50, 73*), mean temperatures for the northern (red line) and southern hemispheres (dashed red line) (*28*) and surface solar radiation (SSR, global dimming in Europe) (*74*). The time delays relate to the recovery of oxidizing capacity for methane and the warming of the ocean for temperatures. Meanwhile CO_2 concentrations (blue line) (*57, 75*) continued to increase monotonically. Temperatures and CO_2 are smoothed with symmetric 5 and 20 year running means, respectively, tapered to 2010. SSR is a polynomial fit to the data.

References and Notes

1. J. Cao, R. Garbaccio, M. Ho, China's 11th Five-Year Plan and the Environment: Reducing SO_2 Emissions, *Rev. Environ. Econ. Policy* **3**, 231 (2009).
2. G. A. Zielinski, P. A. Mayewski, L. D. Meeker, S. Whitlow, M. Twickler, A 110,000-year record of explosive volcanism from the GISP2 (Greenland) ice core, *Quaternary Res.* **45**, 109 (1996) (ftp.ncdc.noaa.gov/pub/data/paleo/icecore/greenland/summit/gisp2/chem/volcano.txt).
3. S. Smith *et al.*, Anthropogenic sulfur dioxide emissions: 1850-2005, *Atmos. Chem. Phys.* **11**, 1101 (2011).
4. A. Van Donkelaar *et al.*, Analysis of aircraft and satellite measurements from the Intercontinental Chemical Transport Experiment (INTEX-B) to quantify long-range transport of East Asian sulfur to Canada, *Atmos. Chem. Phys.* **8**, 2999 (2008).
5. V. Fiedler *et al.*, East Asian SO_2 pollution plume over Europe–Part 1: Airborne trace gas measurements and source identification by particle dispersion model simulations, *Atmos. Chem. Phys.* **9**, 4717 (2009).
6. P. L. Ward, Sulfur dioxide initiates global climate change in four ways, *Thin Solid Films* **517**, 3188 (2009).
7. S. Ramachandran, V. Ramaswamy, G. L. Stenchikov, A. Robock, Radiative impact of the Mount Pinatubo volcanic eruption: Lower stratospheric response, *J. Geophys. Res* **105**, 24409 (2000).
8. M. Planck, *The Theory of Heat Radiation*. (Forgotten Books, 2010, 1912), pp. 244.
9. K. Trenberth, J. Fasullo, J. Kiehl, Earth's global energy budget, *Bull. Am. Meteorol. Soc.* **90**, 311 (2009).
10. R. A. Rohde, *commons.wikimedia.org/wiki/File:Atmospheric_Transmission.png* (2010).

11. J. Tyndall, *Contributions to Molecular Physics in the Domain of Radiant Heat*. (Longmans, Green, and Co., London, 1872), pp. 446, www.archive.org/details/contributionsto00tyndgoog.

12. C. Hermans, A. Vandaele, S. Fally, Fourier transform measurements of SO_2 absorption cross sections: I. Temperature dependence in the 24000–29000cm^{-1} (345–420nm) region, *J. Quant. Spectrosc. Radiat. Trans.* **110**, 756 (2009).

13. A. Vandaele, C. Hermans, S. Fally, Fourier transform measurements of SO_2 absorption cross sections: II. Temperature dependence in the 29000–44000cm^{-1} (227–345nm) region, *J. Quant. Spectrosc. Radiat. Trans.* **110**, 2115 (2009).

14. L. Rothman *et al.*, The HITRAN 2008 molecular spectroscopic database, *J. Quant. Spectrosc. Radiat. Trans.* **110**, 533 (2009).

15. D. C. Harris, M. D. Bertolucci, *Symmetry and Spectroscopy: An Introduction to Vibrational and Electronic Spectroscopy*. (Oxford University Press, 1978), pp. 550.

16. V. Ramanathan, G. Carmichael, Global and regional climate changes due to black carbon, *Nature Geosci.* **1**, 221 (2008).

17. C. Gueymard, The sun's total and spectral irradiance for solar energy applications and solar radiation models, *Solar Energy* **76**, 423 (2004).

18. G. A. Ban-Weiss, L. Cao, G. Bala, K. Caldeira, Dependence of climate forcing and response on the altitude of black carbon aerosols, *Clim. Dynam.* **36**, online (2011).

19. IPCC, *Climate Change 2007: The Physical Science Basis*. S. Solomon *et al.*, Eds. (Cambridge University Press, 2007), pp. 996.

20. V. Fiedler *et al.*, East Asian SO_2 pollution plume over Europe-Part 2: Evolution and potential impact, *Atmos. Chem. Phys.* **9**, 4729 (2009).

21. F. Arnold *et al.*, Observation of upper tropospheric sulfur dioxide and acetone pollution: Potential implications for hydroxyl radical and aerosol formation, *Geophys. Res. Lett.* **24**, 57 (1997).

22. G. J. S. Bluth, S. D. Doiron, C. C. Schnetzler, A. J. Krueger, L. S. Walter, Global tracking of the SO_2 clouds from the June, 1991 Mount Pinatubo eruptions, *Geophys. Res. Lett.* **19**, 151 (1992).

23. W. G. Read, L. Froidevaux, J. W. Waters, Microwave Limb sounder measurement of stratospheric SO_2 from the Mt. Pinatubo Volcano, *Geophys. Res. Lett.* **20**, 1299 (1993).

24. H. Singh, W. Brune, J. Crawford, F. Flocke, D. Jacob, Chemistry and transport of pollution over the Gulf of Mexico and the Pacific: spring 2006 INTEX-B campaign overview and first results, *Atmos. Chem. Phys.* **9**, 2301 (2009).

25. S. M. Kreidenweis, Y. Zhang, G. R. Taylor, The effects of clouds on aerosol and chemical species production and distribution 2. Chemistry model description and sensitivity analysis, *J. Geophys. Res.* **102**, 23867 (1997).

26. A. Ding *et al.*, Transport of north China air pollution by midlatitude cyclones: Case study of aircraft measurements in summer 2007, *J. Geophys. Res* **114** (2009).

27. R. G. Grainger *et al.*, Infrared absorption by volcanic stratospheric aerosols observed by ISAMS, *Geophys. Res. Lett.* **20**, 1293 (1993).

28. HadCRUT3, *www.cru.uea.ac.uk/cru/data/temperature/* (2010).

29. S. Levitus *et al.*, Global ocean heat content 1955–2008 in light of recently revealed instrumentation problems, *Geophys. Res. Lett.* **36**, L07608 (2009).

30. *www.oco.noaa.gov/index.jsp?show_page=page_roc.jsp&nav=universal* (2010).

31. D. W. Lea, D. K. Pak, H. J. Spero, Climate impact of Late Quaternary equatorial Pacific sea surface temperature variations, *Science* **289**, 1719 (2000).

32. M. Hoerling, A. Kumar, J. Eischeid, B. Jha, What is causing the variability in global mean land temperature?, *Geophys. Res. Lett.* **35**, L23712 (2008).

33. G. P. Compo, P. D. Sardeshmukh, Oceanic influences on recent continental warming, *Clim. Dynam.* **32**, 333 (2009).

34. D. Dommenget, The ocean's role in continental climate variability and change, *J. Clim.* **22**, 4939 (2009).

35. P. J. Gleckler *et al.*, Krakatoa lives: The effect of volcanic eruptions on ocean heat content and thermal expansion, *Geophys. Res. Lett.* **33**, L17702 (2006).

36. J. M. Gregory, J. A. Lowe, S. F. B. Tett, Simulated global-mean sea level changes over the last half-millennium, *J. Clim.* **19**, 4576 (2006).

37. A. Grinsted, J. C. Moore, S. Jevrejeva, Observational evidence for volcanic impact on sea level and the global water cycle, *Proc. Nat. Acad. Sci. U.S.A.* **104**, 19730 (2007).

38. *www.espere.net/Unitedkingdom/water/uk_ozone.htm* (2010).

39. P. L. Ward, Understanding volcanoes may be the key to controlling global warming, *Soc. Vac. Coaters Bull.* **Summer**, 26 (2010).

40. T. Thordarson, S. Self, Atmospheric and environmental effects of the 1783–1784 Laki eruption: A review and reassessment, *J. Geophys. Res.* **108**, 4011 (2003).

41. S. Self, S. Blake, K. Sharma, M. Widdowson, S. Sephton, Sulfur and Chlorine in Late Cretaceous Deccan Magmas and Eruptive Gas Release, *Science* **319**, 1654 (2008).

42. ATSDR, Sulfur Dioxide: Medical Management Guidelines, *www.atsdr.cdc.gov/MMG/MMG.asp?id=249&tid=46* (2010).

43. D. Parker, T. Legg, C. Folland, A new daily central England temperature series, 1772-1991, *Int. J. Climatol.* **12**, 317 (1992).

44. *hadobs.metoffice.com/hadcet/data/download.html* (2010).

45. P. A. Mayewski *et al.*, Major features and forcing of high-latitude northern hemisphere atmospheric circulation using a 110,000-year-long glaciochemical series, *J. Geophys. Res.* **102**, 26345 (1997).

46. S. Rahmstorf, Timing of abrupt climate change: A precise clock, *Geophys. Res. Lett.* **30**, 1510 (2003).

47. L. A. Barrie, R. M. Hoff, The oxidation rate and residence time of sulphur dioxide in the arctic atmosphere, *Atmos. Environ.* **18**, 2711 (1984).

48. K. Law, A. Stohl, Arctic air pollution: Origins and impacts, *Science* **315**, 1537 (2007).

49. K. Rahn, Relative importances of North America and Eurasia as sources of Arctic aerosol, *Atmos. Environ.* **15**, 1447 (1981).

50. E. Dlugokencky *et al.*, Observational constraints on recent increases in the atmospheric CH_4 burden, *Geophys. Res. Lett.* **36**, 17 (2009).

51. M. Wild *et al.*, Global dimming and brightening: An update beyond 2000, *J. Geophys. Res.* **114**, D00D13 (2009).

52. Z. Lu *et al.*, Sulfur dioxide emissions in China and sulfur trends in East Asia since 2000, *Atmos. Chem. Phys.* **10**, 8657 (2010).

53. R. D'Arrigo, R. Wilson, B. Liepert, P. Cherubini, On the 'Divergence Problem'in Northern Forests: A review of the tree-ring evidence and possible causes, *Global Planet. Change* **60**, 289 (2008).

54. T. Keller, Direct effects of sulphur dioxide on trees, *Phil. Trans. Roy. Soc. B* **305**, 317 (1984).

55. S. Manninen, S. Huttunen, Response of needle sulphur and nitrogen concentrations of Scots pine versus Norway spruce to SO_2 and NO_2, *Environ. Pollut.* **107**, 421 (2000).

56. R. Nemani *et al.*, Climate-driven increases in global terrestrial net primary production from 1982 to 1999, *Science* **300**, 1560 (2003).

57. R. F. Keeling et al., Carbon Dioxide Research Group, *cdiac.ornl.gov/ftp/trends/co2/maunaloa.co2* (2008).

58. A. Witze, 2010 ties record for warmest year, *Science News* **Feb. 12**, 17 (2011).

59. K. Trenberth, J. Fasullo, Tracking Earth's Energy, *Science* **328**, 316 (2010).

60. J. Hansen *et al.*, Earth's energy imbalance: Confirmation and implications, *Science* **308**, 1431 (2005).

61. L. McInnes, *en.wikipedia.org/wiki/File:Co2-temperature-plot.svg* (2009).

62. R. Weiss, Carbon dioxide in water and seawater: the solubility of a non-ideal gas, *Marine Chem.* **2**, 203 (1974).

63. L. Stott, A. Timmermann, R. Thunell, Southern hemisphere and deep-sea warming led deglacial atmospheric CO_2 rise and tropical warming, *Science* **318**, 435 (2007).

64. H. Fischer, M. Wahlen, J. Smith, D. Mastroianni, B. Deck, Ice core records of Atmospheric CO_2 around the last three glacial terminations, *Science* **283**, 1712 (1999).

65. E. Monnin *et al.*, Atmospheric CO_2 concentrations over the last glacial termination, *Science* **291**, 112 (2001).

66. N. Caillon *et al.*, Timing of atmospheric CO_2 and Antarctic temperature changes across Termination III, *Science* **299**, 1728 (2003).

67. U. Siegenthaler *et al.*, Stable carbon cycle-climate relationship during the late Pleistocene, *Science* **310**, 1313 (2005).

68. M. Mudelsee, The phase relations among atmospheric CO_2 content, temperature and global ice volume over the past 420 ka, *Quat. Sci. Rev.* **20**, 583 (2001).

69. R. McGregor, 750,000 a year killed by Chinese pollution, *Financial Times*, *www.ft.com/cms/s/0/8f40e248-28c7-11dc-af78-000b5df10621.html?nclick_check=1* (2007).

70. B. J. Finlayson-Pitts, J. N. Pitts, *Chemistry of the Upper and Lower Atmosphere: Theory, Experiments, and Applications*. (Academic Press, San Diego, 1999), pp. 969.

71. S. Madronich, The atmosphere and UV-B radiation at ground level in *Environ. UV Photobiology*, A. R. Young, Ed. (Plenum Press, 1993), vol. 1, pp. 39.

72. J. W. C. White *et al.*, The climate signal in the stable isotopes of snow from Summit, Greenland: Results of comparisons with modern climate observations, *J. Geophys. Res.* **102**, 26425 (1997).

73. D. M. Etheridge, L. P. Steele, R. J. Francey, R. L. Langenfelds, Atmospheric methane between 1000 A.D. and present: Evidence of anthropogenic emissions and climatic variability *J. Geophys. Res.* **103**, 15979 (1998).

74. K. Makowski *et al.*, On the relationship between diurnal temperature range and surface solar radiation in Europe, *J. Geophys. Res.* **114**, D00D07 (2009).

75. D. M. Etheridge *et al.*, Historical CO_2 record from the Law Dome DE08, DE08-2, and DSS ice cores, *cdiac.ornl.gov/ftp/trends/co2/lawdome.combined.dat* (1998).

Begin references for supporting online text

76. P. Maroulis, A. Torres, A. Goldberg, A. Bandy, Atmospheric SO_2 measurements on project Gametag, *J. Geophys. Res.* **85**, 7345 (1980).

77. U. S. Environmental Protection Agency, *www.epa.gov/air/airtrends/sulfur.html* (2010).

78. D. Miller, M. Flores, Sulfur dioxide concentrations in western US, *Atmos. Environ.* **26**, 345 (1992).

79. U. S. Environmental Protection Agency, *yosemite.epa.gov/opa/admpress.nsf/6427a6b7538955c585257359003f0230/c045295ced7dcf6885257758005b74bb!OpenDocument* (July 6, 2010).

80. G. Shaw, The Arctic haze phenomenon, *Bull. Am. Meteorol. Soc.* **76**, 2403 (1995).

81. R. Koerner, D. Fisher, Acid snow in the Canadian high Arctic, *Nature* **295**, 137 (1982).

82. D. Thornton, A. Bandy, A. Driedger, Sulfur dioxide in the North American arctic, *J. Atmos. Chem.* **9**, 331 (1989).

83. S. Sharma, D. Lavoué, H. Cachier, L. Barrie, S. Gong, Long-term trends of the black carbon concentrations in the Canadian Arctic, *J. Geophys. Res.* **109**, D15203 (2004).

84. K. Rahn, Progress in Arctic air chemistry, 1980-1984, *Atmos. Environ.* **19**, 1987 (1985).

85. K. Rahn, E. Joranger, A. Semb, T. Conway, High winter concentrations of SO_2 in the Norwegian Arctic and transport from Eurasia, *Nature* **287**, 824 (1980).

86. L. Barrie, D. Fisher, R. Koerner, Twentieth century trends in Arctic air pollution revealed by conductivity and acidity observations in snow and ice in the Canadian high Arctic, *Atmos. Environ.* **19**, 2055 (1985).

87. V. Ramanathan, A. Vogelmann, Greenhouse effect, atmospheric solar absorption and the earth's radiation budget: From the Arrhenius-Langley era to the 1990s, *Ambio* **26**, 38 (1997).

88. M. Ramana, V. Ramanathan, D. Kim, G. Roberts, C. Corrigan, Albedo, atmospheric solar absorption and heating rate measurements with stacked UAVs, *Quat. J. Roy. Meterol. Soc.* **133**, 1913 (2007).

89. F. Valero *et al.*, Absorption of solar radiation by the clear and cloudy atmosphere during the Atmospheric Radiation Measurement Enhanced Shortwave Experiments (ARESE) I and II: Observations and models, *J. Geophys. Res.* **108**, 4016 (2003).

90. *en.wikipedia.org/wiki/Sulfur* (2010).

91. *en.wikipedia.org/wiki/Sea_water* (2010).

92. K. L. Denman *et al.*, Couplings between changes in the climate system and biogeochemistry in *Climate Change 2007: The Physical Science Basis. Contribution of Working Group I to the Fourth Assessment Report of the Intergovernmental Panel on Climate Change,* S. Solomon *et al.*, Eds. (Cambridge University Press, Cambridge, United Kingdom and New York, NY, USA, 2007), pp. 499–587.

93. T. M. Gerlach, H. R. Westrich, R. B. Symonds, Preeruption vapor in magma of the climactic Mount Pinatubo eruption: Source of the giant stratospheric sulfur dioxide cloud in *Fire and mud: Eruptions and lahars of Mount Pinatubo, Philippines,* C. G. Newhall, R. S. Punongbayan, Eds. (Philippine Institute of Volcanology and Seismology and University of Washington Press, 1996), pp. 415-433.

94. S. Self, J.-X. Zhao, R. E. Holasek, R. C. Torres, A. J. King, The atmospheric impact of the 1991 Mount Pinatubo eruption in *Fire and Mud: Eruptions and lahars of Mount Pinatubo, Philippines,* C. G. Newhall, R. S. Punongbayan, Eds. (Philippine Institute of Volcanology and Seismology and University of Washington Press, 1996), pp. 1089-1115.

95. G. J. S. Bluth, C. C. Schnetzler, A. J. Krueger, L. S. Walter, The contribution of explosive volcanism to global atmospheric sulphur dioxide concentrations, *Nature* **366**, 327 (1993).

96. P. Minnis *et al.*, Radiative climate forcing by the Mount Pinatubo eruption, *Science* **259**, 1411 (1993).

97. D. Dolske, D. Gatz, A field intercomparison of methods for the measurement of particle and gas dry deposition, *J. Geophys. Res.* **90**, 2076 (1985).

98. B. Hicks, T. Meyers, C. Fairall, V. Mohnen, D. Dolske, Ratios of dry to wet deposition of sulfur as derived from preliminary field data, *Global Biogeochem. Cycles* **3**, 155 (1989).

99. G. Likens, F. Bormann, L. Hedin, C. Driscoll, J. Eaton, Dry deposition of sulfur: a 23-year record for the Hubbard Brook Forest ecosystem, *Tellus* **42B**, 319 (1990).

100. J. Shannon, D. Sisterson, Estimation of S and NO_x-N deposition budgets for the United States and Canada, *Water, Air, & Soil Pollution* **63**, 211 (1992).

101. S. J. Smith, E. Conception, R. Andres, J. Lurz, "Historical sulfur dioxide emissions 1850-2000: Methods and results" pp. 14 (2004).

102. P. Laj, H. Sigurdsson, S. M. Drummey, M. J. Spencer, J. M. Palais, Depletion of H_2O_2 in a Greenland ice core: implications for oxidation of volcanic SO_2, *Nature* **346**, 45 (1990).

103. D. J. Lary, M. Balluch, S. Bekki, Solar heating rates after a volcanic eruption: The importance of SO_2 absorption, *Quat. J. Roy. Meterol. Soc.*, **120**, 1683 (1994).

104. M. F. Gerstell, J. Crisp, D. Crisp, Radiative Forcing of the Stratosphere by SO_2 Gas, Silicate Ash, and H_2SO_4 Aerosols Shortly after the 1982 Eruptions of El Chichón, *J. Clim.* **8**, 1060 (1995).

105. J. Orphal, A critical review of the absorption cross-sections of O_3 and NO_2 in the ultraviolet and visible, *J. Photochem. Photobiol. A* **157**, 185 (2003).

106. D. H. Ehhalt, Photooxidation of trace gases in the troposphere, *Phys. Chem. Chem. Phys.* **1**, 5401 (1999).

107. J. P. Steffensen *et al.*, High-Resolution Greenland Ice Core Data Show Abrupt Climate Change Happens in Few Years, *Science* **321**, 680 (2008).

108. T. Kobashi, J. P. Severinghaus, J-M Barnola, 4 ±1.5°C abrupt warming 11,270 yr ago identified from trapped air in Greenland ice, *Earth Planet. Sci. Lett.* **268**, 397 (2008).

109. C. Huber *et al.*, Isotope calibrated Greenland temperature record over Marine Isotope Stage 3 and its relation to CH_4, *Earth Planet. Sci. Lett.* **243**, 504 (2006).

110. Z. Liu *et al.*, Transient simulation of last deglaciation with a new mechanism for Bølling-Allerød warming, *Science* **325**, 310 (2009).

111. P. D. Ditlevsen, M. S. Kristensen, K. K. Andersen, The recurrence time of Dansgaard-Oeschger events and limits on the possible periodic component, *J. Clim.* **18**, 2594 (2005).

112. P. Huybers, C. Langmuir, Feedback between deglaciation, volcanism, and atmospheric CO_2, *Earth Planet. Sci. Lett.* **286**, 479 (2009).

113. W. Broecker, S. Barker, A 190‰ drop in atmosphere's $\Delta^{14}C$ during the "Mystery Interval" (17.5 to 14.5 kyr), *Earth Planet. Sci. Lett.* **256**, 90 (2007).

114. D. J. R. Thornalley, S. Barker, W. S. Broecker, H. Elderfield, I. N. McCave, The Deglacial Evolution of North Atlantic Deep Convection, *Science* **331**, 202 (2011).

115. E. D. Galbraith *et al.*, Carbon dioxide release from the North Pacific abyss during the last deglaciation, *Nature* **449**, 890 (2007).

116. *en.wikipedia.org/wiki/Atmosphere* (2010).

117. R. A. Berner, GEOCARBSULF: A combined model for Phanerozoic atmospheric O_2 and CO_2, *Geochim. Cosmochim. Acta* **70**, 5653 (2006).

118. J. Veizer *et al.*, $^{87}Sr/^{86}Sr$, $d^{13}C$ and $d^{18}O$ evolution of Phanerozoic seawater, *Chem. Geol.* **161**, 59 (1999).

119. B. Haq, J. Hardenbol, P. Vail, Chronology of fluctuating sea levels since the Triassic, *Science* **235** 1156 (1987).

120. B. U. Haq, S. R. Schutter, A Chronology of Paleozoic Sea-Level Changes, *Science* **322**, 64 (2008).

121. B. U. Haq, J. Hardenbol, P. R. Vail, Mesozoic and Cenozoic chronostratigraphy and eustatic cycles in *Sea-level Changes: an Integrated Approach*, C. K. Wilgus *et al.*, Eds. (Society of Economic Paleontologists and Minerologists, **Spec. Pub. 42**, 1988), pp. 71-108.

122. C. A. Ross, J. R. P. Ross, Timing and depositional history of eustatic sequences: Constraints on seismic stratigraphy, *Cushman Foundation for Foraminiferal Research* **Spec. Pub. 24**, 137 (1987).

123. J. C. Crowell, Pre-Mesozoic ice ages: Their bearing on understanding the climate system, *Geol. Soc. Am. Spec. Pap.* **192**, 1 (1999).

124. L. A. Frakes, J. E. Francis, J. I. Syktus, *Climate modes of the phanerozoic: the history of the earth's climate over the past 600 million years*. (Cambridge University Press, 2005), pp. 274.

125. J. Veizer, Y. Godderis, L. M. Francois, Evidence for decoupling of atmospheric CO_2 and global climate during the Phanerozoic eon, *Nature* **408**, 698 (2000).

126. D. J. Beerling, C. P. Osborne, W. G. Chaloner, Evolution of leaf-form in land plants linked to atmospheric CO_2 decline in the Late Palaeozoic era, *Nature* **410**, 352 (2001).

127. D. L. Royer, Estimating latest Cretaceous and Tertiary atmospheric CO_2 from stomatal indices in *Causes and Consequences of Globally Warm Climates in the Early Paleogene*, S. L. Wing, P. D. Gingerich, B. Schmitz, E. Thomas, Eds. (Geol. Soc. Amer. Spec. Pap., Boulder, 2003), vol. 369, pp. 79-93.

128. en.wikipedia.org/wiki/Atom (2011).

129. L. de Broglie, Waves and quanta, *Nature* **112**, 540 (1923).

130. A. Einstein, Über einen die Erzeugung und Verwandlung des Lichtes betreffenden heuristischen Gesichtspunkt, *Annalen der Physik* **322**, 132 (1905).

131. A. Noelle *et al.*, UV/Vis+ Spectra Data Base, *www.science-softcon.de/uv-vis.htm* (2010).

132. M. O. Andreae, Ocean-atmosphere interactions in the global biogeochemical sulfur cycle, *Marine Chem.* **30**, 1 (1990).

133. T. Bates, B. Lamb, A. Guenther, J. Dignon, R. Stoiber, Sulfur emissions to the atmosphere from natural sources, *J. Atmos. Chem.* **14**, 315 (1992).

134. H.-F. Graf, J. Feichter, B. Langmann, Volcanic sulfur emission: Estimates of source strength and its contribution to the global sulfate distribution, *J. Geophys. Res.* **102**, 10 (1997).

135. C. Oppenheimer, Ice core and palaeoclimatic evidence for the timing and nature of the great mid-13th century volcanic eruption, *Int. J. Climatol.* **23**, 417 (2003).

136. C. Oppenheimer, Limited global change due to the largest known Quaternary eruption, Toba ~74kyr BP?, *Quat. Sci. Rev.* **21**, 1593 (2002).

Acknowledgments: Thanks to Joe Greene, Zach Hall, Will Happer, Mike MacCracken, Brian Tinsley, Adrienne Ward and especially Peter Molnar for provocative comments.

Supporting Online Material

www.sciencemag.org

Supporting Online Text

Figures S1, S2, S3, S4, S5

References 76-136

Supporting Online Material for

The Primary Role of Solar-Ultraviolet-Energy-Absorbing Gases In Global Climate Change

Peter L. Ward.

correspondence to: peward@wyoming.com

This PDF file includes:

SOM Text

Figs. S1 to S5

Tables S1

SOM Text

Observed Concentrations of SO_2 in the Troposphere

A survey from 57°S to 70°N in the southern Pacific through western Canada in 1978 found that SO_2 levels averaged in the boundary layer and in the free troposphere 0.089 ppbv and 0.122 ppbv in the northern hemisphere, 0.057 ppbv and 0.090 ppbv in the southern hemisphere, 0.112 ppbv and 0.160 ppbv over continents, and 0.054 ppbv and 0.085 ppbv over oceans (*76*). But values downwind from anthropogenic pollution sources are much higher.

In the United States, national trends in SO_2 concentrations from 141 sites show a decrease in the average from 11.9 ppbv in 1980 to 3.4 ppbv in 2008 with 95% of the data falling between the dashed lines in Figure S1 (*77*). In 1987, SO_2 concentrations in western states were generally 10 times greater than the concentrations of the marine-air boundary layer to the west and 10-30 times less than the rural concentrations in the eastern U.S. (*78*). In 2010, the U.S. Environmental Protection Agency proposed a rule change that by 2014 would reduce SO_2 emissions by 71% from 2005 levels (*79*).

In Chinese cities, SO_2 concentrations ranged from 43.2 ppbv in 1981 to 19.8 ppbv in 2005 (Figure S2)(*1*). Much of this decrease resulted from building taller smokestacks that help lift the pollution above the local boundary layer and spread it over much larger areas.

SO_2 in the Arctic

SO_2 pollution is a particularly severe problem in the Arctic (*80*) where Arctic haze has formed especially since 1950 (*81*) with levels of SO_2 up to 15 ppbv (*82*) and high

levels of black carbon (*83*). "During the Arctic winter, low temperature, low moisture, and low light intensity effectively prevent rapid photochemically driven conversion of SO_2 to sulfuric acid aerosol"(*82*). The haze forms dominantly during February through April at elevations up to 3 km (*80*) from anthropogenic source regions dominantly in the former Soviet Union and its allies but also from northern Europe and mid-western North America (*84*). SO_2 appears to be swept into the Arctic by cyclonic systems with path lengths of hundreds to thousands of kilometers and SO_2 residence times of at least one week (*85*). Between 1952 and 1977, Arctic air pollution increased 75% while pollution in Europe doubled (*86*).

The polluted air mass covers all the area north of the Arctic circle with two giant lobes extending over Eurasia and North America, an area as large as the African Continent (*80*). Local concentrations of SO_2, black carbon, and other pollutants vary widely as air currents change.

Models Under-Predict Solar Absorption

Atmospheric radiative transfer models typically under-predict observed absorption of solar radiation by up to 8% (*87*, *88*). None of these models include absorption of solar ultraviolet radiation by SO_2. The most detailed studies of this effect have been carried out in north central Oklahoma (*89*) and in the vicinity of the Maldives (*88*) where SO_2 concentrations are typically less than a few ppbv. Finding agreement among the dozens of studies may require accounting for changes in SO_2 concentrations in time (Figure 6) and space.

Anthropogenic Sulfur More Than Doubled the Natural Sulfur Cycle

Sulfur is the tenth most abundant element in our galaxy, eighth most abundant in the human body, and sixth most abundant in Earth's oceans and atmosphere (*90*). Sulfur is an essential component of all living cells and a major nutrient required for the growth of plants and the animals that consume them. The biosphere depends on the constant availability of trace amounts of sulfur. Sulfur is the major cause of acidity in rain and sulfate ($SO_4^=$) is the second most common anion after chlorine (Cl^-) in both fresh and salt water (*91*). Sulfur from the earth's interior enters the biosphere typically as sulfur dioxide gas (SO_2) emitted from sub-aerial volcanoes in an oxygen-rich environment and hydrogen sulfide gas (H_2S) emitted from sub-marine volcanoes in an anoxic environment. The natural and anthropogenic emissions of sulfur into the atmosphere each year are estimated in Table S1.

The natural sulfur cycle involves circulating 27 to 59 Mt sulfur per year through the atmosphere. By 1979, anthropogenic sulfur emissions reached 68.3 Mt/year (*3*), increasing this cycle by a factor of 1.16 to 2.5 while CO_2 emissions were increasing the much larger carbon cycle (*92*) by a mere factor of 0.15.

SO_2 and Sulfate Aerosols

During the climactic eruption of Mt. Pinatubo on June, 1991, 17±2 Mt SO_2 (*93*) was injected within 9 hours into the most concentrated part of the ozone layer (altitude 20-25 km), where stratospheric winds spread it around the earth in 21 days (*94*). Within 35 days, ~37% of the SO_2 had been converted to an aerosol (*95*) (nominally 75% H_2SO_4, 25% H_2O) with particle sizes growing to 0.3-0.5 μm within a few months. Ultimately the

volume of aerosol observed required conversion of only 13 Mt of the SO_2 erupted (*94*). Unoxidized SO_2 was observed in the lower stratosphere up to 170 days after the eruption.

By August, this aerosol increased total atmospheric optical depth by a factor of 5 to ~0.35, reducing insolation globally ~2.7 W/m^2 (0.2%), lowering mean surface temperatures ~0.5^oC, decaying exponentially until negligible in 1995 (*96*). Meanwhile the gas and aerosol absorbed enough dominantly solar energy to warm the lower stratosphere ~3^oC. Formation of the aerosol and its effectiveness in cooling depended on the availability of ample ozone, of ample ultraviolet radiation with wavelength <0.32 μm to initiate the formation of OH from ozone, and of horizontal stratospheric winds with minimal vertical turbulence to allow growth of the particles and efficient spreading of the aerosol worldwide.

SO_2 is removed from the lower troposphere either by oxidation and subsequent wet deposition or by dry deposition. Dry deposition is "the removal of particles or gases from the atmosphere through the delivery of mass to the surface by non-precipitation atmospheric processes, and the subsequent chemical reaction with, or physical attachment to, vegetation, soil, or the built environment" (*97*). Near ground turbulence essentially "paints" SO_2 onto the surfaces of structures, leaves, needles, grass, snow, water, etc. The SO_2 is then oxidized to acid on these surfaces, appearing as if fallen in acid rain.

In climates outside of the tropics, dry deposition of SO_2 appears to be the dominant process in the lower troposphere. Studies in Tennessee, New York, and Illinois found the ratio of dry deposition to wet deposition to be 0.3 in summer but 2.0 for rest of the year (*98*). Yet other studies in New Hampshire showed that dry deposition is dominant during the summer when the deciduous canopy is leafed out (*99*). Dry deposition of sulfur is

slightly greater than wet deposition in the eastern United States, less important in the trans-Mississippi states, and dominant in the western United States (*100*).

Wet deposition carries pollutants farther, perhaps because it nucleates at higher elevations; studies in the northeastern US found that 45% of the particulate sulfur collected on air-flow filters came from distant mid-western sources, whereas 85% of the sulfur in samples of rainwater came from these distant sources (*99*). Furthermore, in this region 37% of the total sulfur emissions remained in the troposphere until over the Atlantic Ocean (*100*).

Dry deposition is dominant in dry climates and becomes more dominant even in wetter climates as the concentration of SO_2 increases, demonstrating the effect of a limited supply of oxidants. For example, in New Hampshire, dry deposition contributed about 12% of total sulfur deposition in 1964-65 but 61% in 1983-84 (*99*) when global emissions had increased by 17% (*101*).

Sulfate in the snow of Greenland is typically associated with local depletion of H_2O_2, suggesting SO_2 reached Greenland as a gas and was oxidized either as precipitation formed locally or after it had been "painted" onto the snow (*102*).

The importance of dry deposition, the observation of sulfate in Greenland from northern Europe and central North America, the extent of "dry fog" observed after the eruption of Laki in 1783 and the detection of SO_2 from China 20,000 km to the east near Ireland (*5*) all demonstrate that under certain conditions, SO_2 can remain in the troposphere for more than two weeks.

The lifetime of SO_2 in the troposphere is most likely extended by lofting, the heating of the gas by absorption of solar ultraviolet radiation, causing it to rise (*103*). Lofting

may also prolong the life of the sulfuric acid aerosol in the lower stratosphere, possibly leading to growth in particle size (*104*). Lofting needs to be included in atmospheric modeling.

Absorption Cross Section for NO_2

Concentrations of nitrogen dioxide (NO_2) from internal combustion engines and thermal power stations can become significant in polluted environments and add to local heating. Absorption is strong at ultraviolet and visible wavelengths (Figure S3) (*105*) and must be included when modeling polluted environments. Small amounts of NO_x have a profound effect on OH concentrations and on the generation of O_3 in the lower troposphere that increase absorption (*106*).

Abrupt Climate Warmings

The 14 Dansgaard-Oeschger abrupt warmings between 48,000 and 11,000 BP (*46*) warmed Summit Greenland as much as 15^{o}C within a few years (*107, 108*) to a few decades but typically cooled back to ice-age conditions over several centuries (*109*). Studies of deep-sea cores suggest these warmings are contemporaneous with major shifts in the Atlantic meridional overturning circulation possibly caused by sudden influx of fresh water into the North Atlantic from glacial lakes or iceberg calving Heinrich events, but neither are contemporaneous with the major Bolling or Preboreal warmings. Sudden warming might be caused by some instability in the climate system (*110, 111*), but major volcanism is the most logical cause for these random (*111*) events as shown in Figure 4 of the main paper and in more detail elsewhere (*6*). Most of these large eruptions would

have occurred under continental ice sheets. Rapid melting of ice would not only provide fresh water to the thermohaline circulation but could cause sudden reduction of pressure on top of crustal magma chambers leading to increased and more continuous volcanism (*112*). Basaltic eruptions in Iceland were common throughout this period and would have been particularly effective increasing tropospheric pollution implicated in warming.

Sudden mixing of ^{14}C-depleted water has also been invoked to explain rapid decreases in the ratio of ^{14}C to C ($\Delta^{14}C$ in Figure S4) (*113-115*), but the apparent contemporaneity with volcanic sulfate per century (red line) suggests that eruption of significant volumes of CO_2, the second most voluminous volcanic gas after water vapor, may have played a major role in causing observed depletion. The most direct way to affect the ocean thermohaline circulation is warming the troposphere through layers of volcanic pollution absorbing ultraviolet and visible energy both directly from the sun and reflected from the surface of the snow.

Can CO_2 be a Primary Cause of Global Warming?

The physics of global warming discussed in the main paper casts doubt on the widespread assumption that CO_2 and other greenhouse gases are a primary cause of global warming:

1. There is far less energy in the infrared bands (Figure 1), not enough to cause electronic transitions that absorb the largest amounts of energy.
2. CO_2 is a linear molecule without a permanent electric dipole, limiting the interaction of individual molecules with the electromagnetic field.

3. Absorption of CO_2 involves spectral lines (Figure 2), not a continuum, implying much less net absorption of energy.

CO_2 is assumed to be the most important greenhouse gas because it has the highest concentration of any radiatively-active gas in the atmosphere, except for water vapor. Concentrations of CO_2 are low during glacial periods and high during non-glacial periods, but cold water absorbs more CO_2 (*62*). If CO_2 is a primary cause of warming and warming causes significant amounts of CO_2 to leave the oceans, why is there not runaway warming?

CO_2 makes up only 0.039% of the atmosphere while water vapor averages 0.247% (*116*), 6.3 times greater. Water absorbs energy at many more wavelengths than CO_2, even at solar wavelengths (Figure 1). Water is an aspherical top molecule with a permanent electric dipole. Water should be the most important greenhouse gas, possibly even by several factors of ten. Concentrations of water vapor are greatest in the tropics and least at the poles, but global warming is least in the tropics and greatest at the poles. Does absorption of infrared energy by water vapor really generate that much heat?

Figure S4 shows the variation of CO_2 (red line) (*117*), the $\delta^{18}O$ proxy for temperature (green line and shading) (*118*), and sea-level (blue line) (*119-122*) for the past 600 million years. Glacial deposits are observed in large parts of the world at times when the temperatures were to the left of the vertical green line (*123*, *124*). There were four epochs of glaciation (numbers) that do not show a direct correlation with low concentrations of CO_2. The correlation of sea-level and temperature with time is much stronger than the correlation between temperature and CO_2 (*125*). The temperature and sea-level data are determined quite precisely at this scale from voluminous data. The CO_2

data are based on sound reasoning and checked against rock types (*117*) and measurements of stomata in fossil leaves (*126, 127*) but are less precisely known.

CO_2 does have an effect on warming, but it has yet to be proven by direct experiments that increased atmospheric concentrations of CO_2 are the primary cause of global warming. Most evidence is circumstantial based on observations and models that assume greenhouse gases are the only cause of observed warming.

The Microphysics of Absorption and Emission

The volume of an atom is 10^{12} times larger than the volume of its nucleus (*128*). Thus, an atom consists almost entirely of oscillating negative electric charge traditionally viewed as electrons moving in orbitals or, according to de Broglie (*129*), as oscillating, three-dimensional, standing waves confined by Coulomb attraction to the nucleus. Spherical standing waves have certain natural, resonant frequencies (normal modes) of oscillation for each spatial degree of freedom determined by the structural properties of the atom. The lowest resonant frequency is the fundamental; higher frequency overtones are separated by half-wavelength increments (electronic transitions). Planck (*8*) postulated that energy (E) in electromagnetic radiation (EMR) is equal to Planck's constant (h) times frequency (ν) ($E=h\nu$). Thus the fundamental frequency can be thought of as the ground state of the valance standing wave (electron) and higher frequency standing waves as higher energy, electronically excited states. The energy differences between these normal modes are the energy quanta of quantum mechanics. When this standing wave is induced to oscillate at a frequency with energy high enough to

overcome Coulomb attraction of the nucleus, the standing wave (electron) exits the atom causing the photoelectric effect, a function of frequency but not intensity (*130*).

Molecules similarly oscillate at specific resonant frequencies determined by the structural properties of the molecule (vibrational transitions). The forces binding the atoms are electromagnetic but can be thought of as acting like springs that oscillate in symmetric stretch, asymmetric stretch and bending modes creating normal modes of oscillation for each degree of freedom for each chemical bond.

Molecules also have moments of inertia about three orthogonal axes absorbing energy when the molecule tries to stay aligned to an oscillating electromagnetic field (rotational transitions). The field exerts a torque on triatomic, asymmetric top molecules such as water, ozone, SO_2, and NO_2 with permanent electric dipoles. The field interacts much less effectively with linear molecules such as CO_2 that can only have induced electric dipoles and very little with diatomic molecules such as nitrogen. Microwave ovens use forced oscillation of dipole rotation to heat water much more efficiently than fats and sugars.

Temperature is the average kinetic energy of all of these atomic and molecular oscillations. Energy increases as a function of a constant times temperature in Kelvin raised to the fourth power (Stefan-Boltzmann law). Temperature does not exist in a vacuum. Temperature of a gas is often thought of as the kinetic energy of translation of molecules, but this is likely a result of a temperature increase rather than its cause: molecules oscillating at higher intensities and higher frequencies will impart more translational energy during collisions with other molecules depending on the phase

difference between the internal oscillations of the two molecules at the instant of collision.

Electric charge in atoms and molecules induces an electric field in the vacuum of space. Oscillating electric charge induces a perpendicular magnetic field that induces a perpendicular electric field, etc., forming, in essence, a perpetual motion machine without mass or friction. Electromagnetic energy propagates through space without loss until it interacts with matter. The universe thus consists of a field of oscillating negative electric charge continuous throughout both space and the vast majority of the volume of matter. This field varies widely in spectral amplitudes (intensities) set by the dynamic sum of the internal oscillations within all matter, all spectral amplitudes of all radiation emitted by matter minus all spectral amplitudes absorbed by matter. In effect, the luminiferous aether sought in the late 19^{th} century is light (EMR) itself and the velocity of light is the velocity that an energy disturbance travels in this aether of massless oscillations.

The flow of energy in this aether occurs through resonance at each specific frequency from higher intensity (amplitude) to lower intensity (higher temperature to lower temperature). When the spectral intensity is higher in matter, these oscillations will induce resonance of similar frequencies in space, emitting radiation. When the spectral intensities of radiation in space are greater than the natural frequencies of oscillation in matter, they will induce resonance of the natural frequencies in matter, causing the matter to absorb energy. Within matter, energy flows by conduction involving both resonance and the flow of electrons. This resonance has a very high Q-factor as shown by the narrowness of spectral lines of absorption observed for vibrational and rotational transitions and utilized through spectroscopy at local to intergalactic distances to identify

the specific molecules causing absorption (*14*). Similarly for UV-Vis spectroscopy (*131*). Planck's law for black body radiation as a function of temperature was derived assuming a "system of resonators" where E=hν (*8*).

E=hν makes good physical sense because EMR consists solely of frequency of oscillation and it is the frequency that does the work on the absorbing molecule. But this simple relationship is counterintuitive for those familiar with waves in matter where matter provides the restoring force for the disturbance. In matter, the energy radiated is proportional to the amplitude (intensity) squared and is attenuated with distance. Waves in matter constructively and destructively interfere, changing the amplitude and frequency. Waves of EMR superpose, normally changing the spectral intensity only; a red light appears red no matter what the intensity.

Rotational transitions with energies <0.074 eV are the only transitions occurring at wavelengths between ~17 and ~100 μm (mid to far-infrared) (Figure 1). Vibrational transitions become important at energies >0.074 eV and are usually coupled with the much smaller rotational transitions. Electronic transitions become important at wavelengths <~1 μm (near-infrared) with energies >1.24 eV and are usually coupled with the much less energetic vibrational and rotational transitions (rotovibronic transitions). There are 5 types of electronic transitions in 4 bands superimposed on other molecular energy states causing absorption along a continuum instead of spectral lines typical for rotational and vibrational transitions.

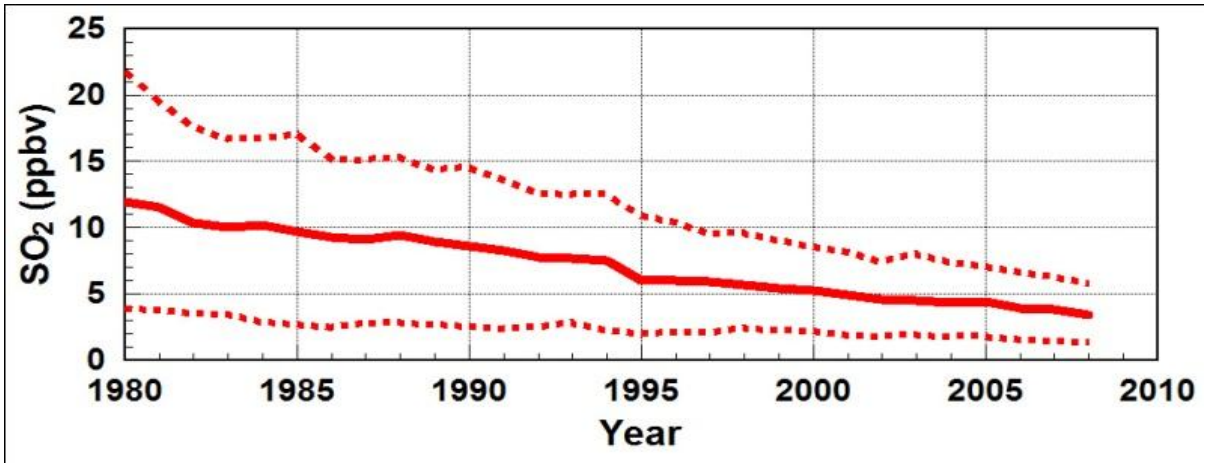

Fig. S1.

U.S. national trends in SO_2 levels based on measurements within meters of the ground at 141 sites.

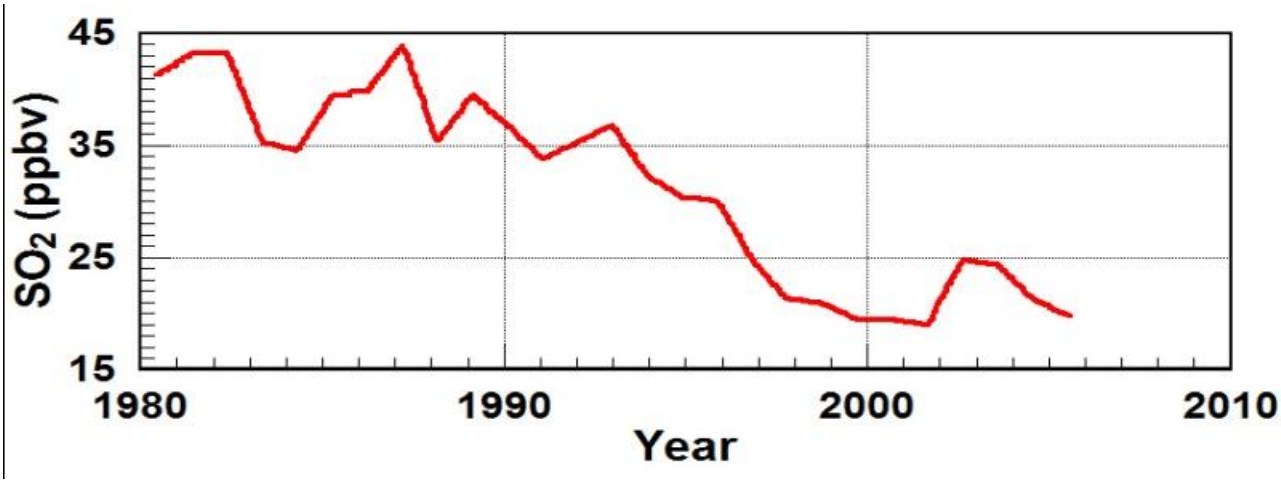

Fig. S2.

Average SO_2 concentrations in up to 113 Chinese cities.

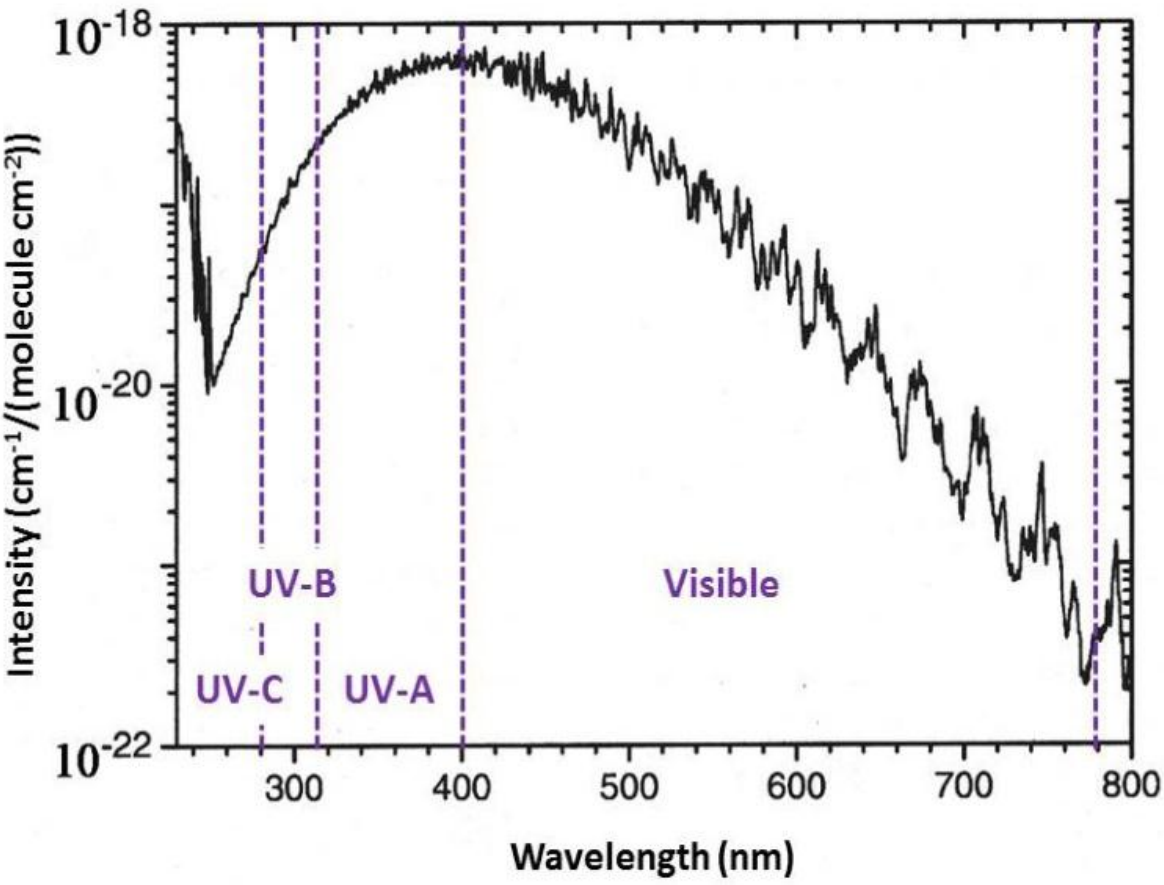

Fig. S3.

Absorption cross section for NO_2.

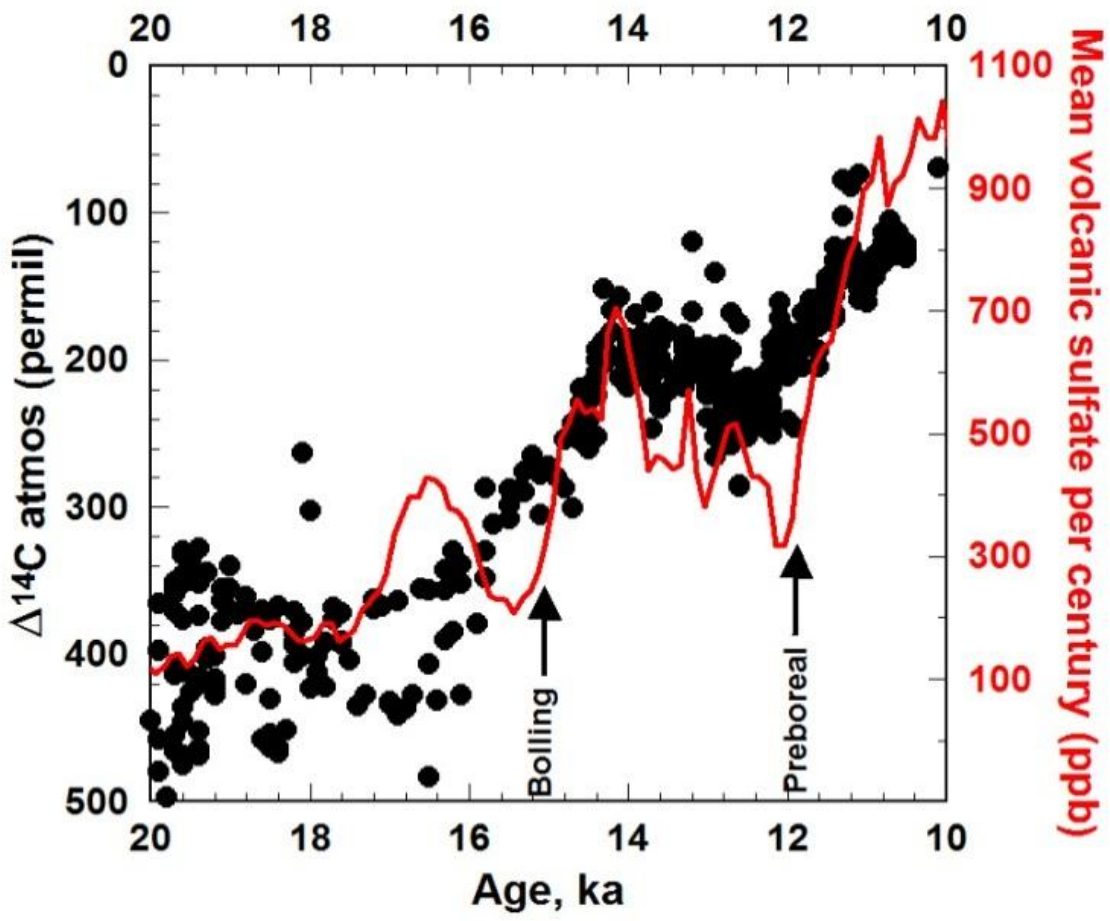

Fig. S4.

Rapid decreases in the ratio of ^{14}C to C ($\Delta^{14}C$) (*113*) are contemporaneous with rapid increases in volcanic sulfate deposited in Greenland suggesting eruption of CO_2**.**

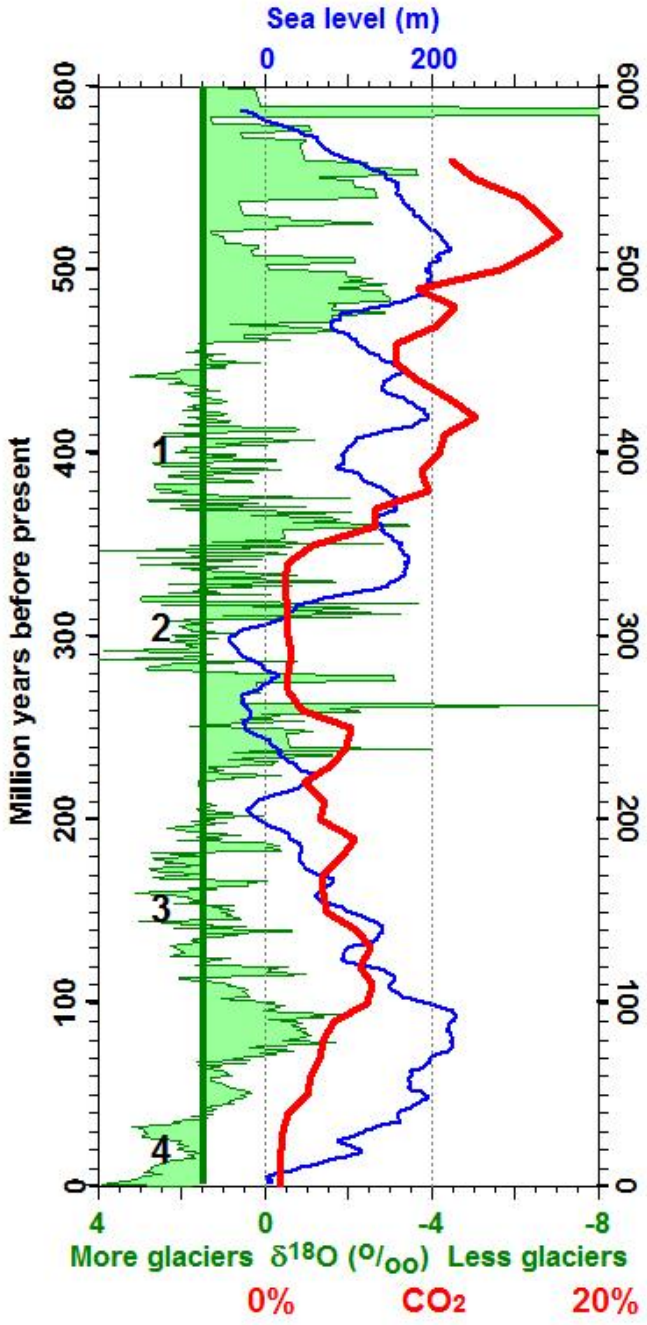

Fig. S5.

CO_2 concentrations (red line) in the atmosphere were low only during two of the four major epochs of glaciation (numbers). The green shaded areas show a proxy for temperature. The blue line shows sea level.

Natural Emissions	**Teragrams Sulfur Per Year**	**Reference**
Oceanic, DMS	15-35	(*132*)
Oceanic, H_2S	2.9	(*132*)
Oceanic, OCS	0.3	(*132*)
Oceanic, CS_2	0.2	(*132*)
Continental Biogenic	0.2	(*133*)
Biomass Burning	0.1	(*133*)
Volcanic Background	8-20	(*134*)
Total	**27-59**	
Anthropogenic Emissions		
2005	59.8	(*3*)
1979	68.3	(*3*)
1965	54.6	(*3*)
1950	30.1	(*3*)
1900	11.4	(*3*)
1850	2.3	(*3*)
Biomass burning	2.1	(*133*)
Specific Volcanic Eruptions		
El Chichón, 1982	3.5	(*22*)
Pinatubo, 1991	8.5	(*93*)
Tambora, 1815	60	(*135*)
Laki, 1783	61	(*40*)
Toba, ~74,000 BP	>570	(*136*)

Table S1.

Natural and anthropogenic emissions of sulfur into the atmosphere per year.